18th Australasian Fluid Mechanics Conference
Launceston, Australia
3-7 December 2012

Thermo-magnetic convection of paramagnetic fluids with non-instantaneous heating

S. C. Saha and Y. T. Gu

School of Chemistry, Physics and Mechanical Engineering
Queensland University of Technology
2 George Street, Brisbane, QLD - 4001, Australia

Abstract

The unsteady boundary-layer development for thermo-magnetic convection of paramagnetic fluids inside a square cavity has been considered in this study. The cavity is placed in a microgravity condition (no gravitation acceleration) and under a uniform magnetic field which acts vertically. A ramp temperature boundary condition is applied on left vertical side wall of the cavity where the temperature initially increases with time up to some specific time and maintain constant thereafter. A distinct magnetic convection boundary layer is developed adjacent to the left vertical wall due to the effect of the magnetic body force generated on the paramagnetic fluid. An improved scaling analysis has been performed using triple-layer integral method and verified by numerical simulations. The Prandtl number has been chosen greater than unity varied over 5-100. Moreover, the effect of various values of the magnetic parameter and magnetic Rayleigh number on the fluid flow and heat transfer has been shown.

Introduction

In nature, natural convection occurs everywhere in the gravitational field. The important areas of interest in studying natural convection include the field of oceanography, geophysics, meteorology, astrophysics, energy systems, material science, etc. It is found in the literature that many resrearchers are interested in this topic because of its fundamental interest in fluid mechanics and practical applications. The differentially heated cavity is a classical example where the fluid adjacent to the heated wall undergoes motion as a result of heat being transferred from the wall into the fluid. It is noted that the hot fluid reduces its density and rises relative to the ambient colder fluid.

It is well known that for natural convection the driving force is usually the density difference as a result of the temperature difference between two fluid zones. However, the fluid will experience a magnetic force if the fluid itself is subject to a magnetic field, which depends on the magnetic susceptibility. Braithwaite et al. [1] showed that from the superconducting magnets the strong magnetic fields could be used to induce magnetic convection in normal paramagnetic fluids. Based on their experimental studies, authors showed that the magnetic field could enhance or suppress the gravitational convection. It might be a interesting topic to be investigated because of the availability of the superconducting magnet. The benefits might be to manage the heat transfer or to control microstructure in crystal growth.

Kaneda et al. [2] studied the effect of the gradient magnetic field with a four-pole electric magnet. Using a method similar to the Boussinesq approximation, Tagawa et al. [3] derived a model equation for magnetic convection for both air and water. The numerical simulations revealed many interesting results for both differentially heated cubic cavity and the Rayleigh Benard convection in the shallow cylinder. Bednarz et al. [4, 5] have shown both numerically and experimentally how to enhance or suppress heat transfer by placing the magnet at various positions of the enclosure.

Governing equations and geometry considered

The governing equations of motion for electrically non-conducting paramagnetic thermo-fluids subject to a magnetic field, together with the temperature equation, can be written in the following two-dimensional form:

$$\frac{\partial u}{\partial x}+\frac{\partial v}{\partial y}=0 \tag{1}$$

$$\frac{\partial u}{\partial t}+u\frac{\partial u}{\partial x}+v\frac{\partial u}{\partial y}=-\frac{1}{\rho}\frac{\partial p}{\partial x}+\nu\left(\frac{\partial^2 u}{\partial x^2}+\frac{\partial^2 u}{\partial y^2}\right) -\frac{\chi_0(\beta+1/T_0)}{2\mu_m}(T-T_0)\frac{\partial b^2}{\partial x} \tag{2}$$

$$\frac{\partial v}{\partial t}+u\frac{\partial v}{\partial x}+v\frac{\partial v}{\partial y}=-\frac{1}{\rho}\frac{\partial p}{\partial y}+\nu\left(\frac{\partial^2 v}{\partial x^2}+\frac{\partial^2 v}{\partial y^2}\right) -\frac{\chi_0(\beta+1/T_0)}{2\mu_m}(T-T_0)\frac{\partial b^2}{\partial y} \tag{3}$$

$$\frac{\partial T}{\partial t}+u\frac{\partial T}{\partial x}+v\frac{\partial T}{\partial y}=\kappa\left(\frac{\partial^2 T}{\partial x^2}+\frac{\partial^2 T}{\partial y^2}\right) \tag{4}$$

where u and v are the $x-$direction and $y-$direction velocity components respectively, t the time, p the pressure, T the temperature, and β, ν and κ are respectively the thermal expansion coefficient, the kinematic viscosity and the thermal diffusivity of the fluid at T_0. μ_m is the magnetic permeability, χ the magnetic susceptibility, ρ the density of the fluid. The details derivation of the last terms of equations (2) and (3) can be found in the work of Braithwaite et al [1] and Bednarz et al. [5].

Under consideration is the transient flow behaviour resulting from heating a quiescent, isothermal Newtonian fluid with $Pr > 1$ in a two-dimensional open cavity of height H by imposing a ramped temperature, T_p defined below, on the left vertical wall, in the absence of gravity but in the presence of a magnetic field, as shown in Fig. 1.

$$T_p=\begin{cases} T_0 & \text{if } t<0 \\ T_0+\Delta T\left(\frac{t}{t_p}\right) & \text{if } 0\le t<t_p \\ T_0+\Delta T & \text{if } t\ge t_p \end{cases} \tag{5}$$

where ΔT is the global temperature difference and t_p is length of the ramp time. The fluid is assumed initially at rest with the uniform temperature T_0 ($T_0 < T_p$). The heat transferred by conduction through the left wall leads to an increase in the temperature of the fluid adjacent to the wall which changes the magnetic susceptibility of the paramagnetic fluid, resulting in a magnetic buoyancy force within the fluid. The top and the bottom walls are kept adiabatic and the right boundary is kept open,

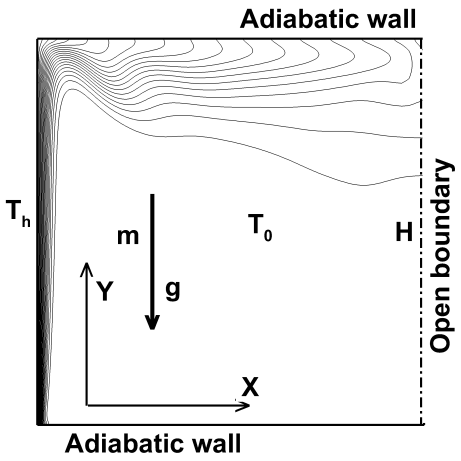

Figure 1: Temperature contours of a typical case and boundary conditions with cordinate system

where the first derivatives of temperature, velocities, and pressure are all assumed to be zero. All boundaries except the right boundary are nonslip. It is also assumed that the flow is laminar. The fluid is assumed to be subject to a uniform, vertical gradient magnetic field (i.e., it is assumed that $\partial(b^2)/\partial x = 0,\ \partial(b^2)/\partial y$ constant). The problem becomes similar to the transient gravitational natural convection flow in a differentially heated cavity by using the assumption for the vertical gradient magnetic field.

Scaling analysis

Boundary layer development stage

The energy equation (4) indicates that since the fluid is initially quiescent the heating effect of the wall will first diffuse into the fluid layer through pure conduction, resulting in a thermal boundary layer of thickness δ_T. Within the boundary layer, the dominant balance is between the unsteady and diffusion terms in the energy equation (4), which gives,

$$\delta_T \sim \kappa^{1/2} t^{1/2}, \tag{6}$$

This scaling is valid until the convection term becomes important.

For $Pr \gg 1$, the unsteady term is much smaller than the viscous term [5] and the correct balance is between the viscosity and the buoyancy; that is,

$$0 \sim \nu \frac{\partial^2 v_m}{\partial x^2} - \frac{\chi_0(\beta + 1/T_0)}{2\mu_m} \Delta T \left(\frac{t}{t_p}\right) \frac{\partial(b^2)}{\partial y}, \tag{7}$$

In both regions I and II in Figure 2, the initial balance in the vertical momentum equation is between the buoyancy and viscous terms, so long as the scale (6) holds.

The peak velocity v_m occurs within the thermal boundary layer δ_T at a distance δ_{vm} from the wall. Also, there will be a region of flow outside δ_T where the flow is not directly forced by buoyancy, but is instead the result of diffusion of momentum via viscosity. This occurs up to a distance δ_v from the wall.

In regions I and II, the balance is between viscosity and buoyancy. However, in region III the balance is between viscosity and inertia, since there is no buoyancy there. In region I, the

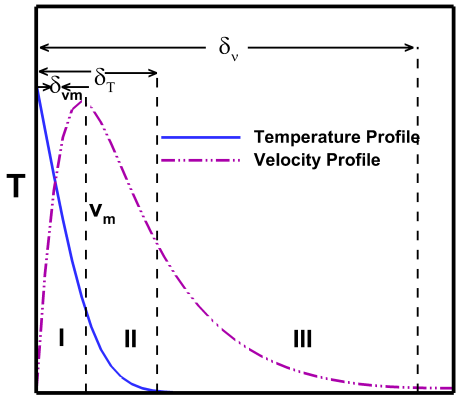

Figure 2: A schematic of the temperature and vertical velocity profiles on the line perpendicular to the left wall at its mid point

balance (7) gives:

$$\nu \frac{v_m}{\delta_{vm}^2} \sim \frac{\chi_0(\beta + 1/T_0)\Delta T}{\mu_m} \left(\frac{t}{t_p}\right) \frac{\partial(b^2)}{\partial y}, \tag{8}$$

which yields

$$v_m \sim \frac{\chi_0(\beta + 1/T_0)\Delta T}{\nu \mu_m} \left(\frac{t}{t_p}\right) \frac{\partial(b^2)}{\partial y} \delta_{vm}^2, \tag{9}$$

In region II, the forcing is over distance $(\delta_T - \delta_{vm})$, but the gradient of the velocity is over $(\delta_v - \delta_{vm})$. Therefore, a suitable scaling analysis would be to integrate relation (7) over region II:

$$0 \sim \nu \frac{\partial v}{\partial x}\Big|_{\delta_{vm}}^{\delta_v} - \frac{\chi_0(\beta + 1/T_0)}{\mu_m} \left(\frac{t}{t_p}\right) \frac{\partial(b^2)}{\partial y} \int_{\delta_{vm}}^{\delta_T} T dx, \tag{10}$$

Since $\partial v/\partial x|_{\delta_{vm}} = 0$ [since the velocity is maximum there] we have

$$\frac{\partial v}{\partial x}\Big|_{\delta_{vm}}^{\delta_v} \sim \frac{v_m}{\delta_v - \delta_{vm}}, \tag{11}$$

and

$$\int_{\delta_{vm}}^{\delta_T} T dx \sim \Delta T(\delta_T - \delta_{vm}). \tag{12}$$

This gives,

$$\nu \frac{v_m}{\delta_v - \delta_{vm}} \sim \frac{\chi_0(\beta + 1/T_0)\Delta T}{\mu_m} \left(\frac{t}{t_p}\right) \frac{\partial(b^2)}{\partial y} (\delta_T - \delta_{vm}). \tag{13}$$

Hence

$$v_m \sim \frac{\chi_0(\beta + 1/T_0)\Delta T}{\nu \mu_m} \left(\frac{t}{t_p}\right) \frac{\partial(b^2)}{\partial y} (\delta_T - \delta_{vm})(\delta_v - \delta_{vm}). \tag{14}$$

Matching this with equation (9) obtained above for v_m gives

$$(\delta_T - \delta_{vm})(\delta_v - \delta_{vm}) \sim \delta_{vm}^2, \tag{15}$$

which implies

$$\delta_T \delta_v - (\delta_T + \delta_v)\delta_{vm} + \delta_{vm}^2 \sim \delta_{vm}^2, \tag{16}$$

finally

$$\delta_{vm} \sim \frac{\delta_T \delta_v}{\delta_T + \delta_v}. \tag{17}$$

In the region III, as there is no buoyancy force, the flow is driven solely by diffusion of momentum, meaning that the unsteady term balances the viscous term which gives,

$$\delta_v \sim Pr^{1/2}\delta_T, \tag{18}$$

which is the scaling of δ_v at the start-up stage. Hence scaling (17) becomes.

$$\delta_{vm} \sim \frac{\kappa^{1/2} t^{1/2}}{1+Pr^{-1/2}}, \tag{19}$$

consequently

$$\delta_T - \delta_{vm} \sim \delta_T - \frac{Pr^{1/2}}{1+Pr^{1/2}}\delta_T \sim \frac{\kappa^{1/2} t^{1/2}}{1+Pr^{1/2}}. \tag{20}$$

So scaling (14), v_m becomes

$$v_m \sim \frac{\chi_0(\beta + 1/T_0)\Delta T}{\nu\mu_m}\left(\frac{t}{t_p}\right)\frac{\partial(b^2)}{\partial y}\left(\frac{1}{1+Pr^{-1/2}}\right)^2 \kappa t, \tag{21}$$

which leads to

$$v_m \sim (\gamma Ra)\frac{m\kappa^2}{H^3}\left(\frac{1}{1+Pr^{-1/2}}\right)^2 \frac{t^2}{t_p}, \tag{22}$$

where

$$m = 1 + \frac{1}{\beta T_0},\ \gamma = \frac{\chi_0 b_0^2}{\mu_m g H} \text{ and } \gamma Ra = \frac{\chi_0 b_0^2 \beta \Delta T H^2}{\mu_m \nu \kappa}, \tag{23}$$

Equation (22) is the scaling for v_m at the start-up stage. In the above equation (23), m is the momentum parameter for paramagnetic fluid, γ is the strength of the magnetic forcing acting on the system and γRa is the magnetic Rayleigh number. The flow in the period that the initial thermal balance is between conduction and unsteady temperature growth is then described by the length scales (6) and (18), and the velocity scale (22). The temperature is described by the scale $O(\Delta T t/t_p)$, so long as $t < t_p$.

Quasi-steady mode

The boundary layer flow is also convecting heat away, and the boundary layer growth will change character when the convection balances conduction, that is, at time t_0 when

$$v_m \frac{\Delta T}{y}\left(\frac{t}{t_p}\right) \sim \kappa \frac{\Delta T}{\delta_T^2}\left(\frac{t}{t_p}\right), \tag{24}$$

which gives

$$v_m \sim \frac{y}{t}. \tag{25}$$

Applying (22), the relation (25) becomes

$$(\gamma Ra)\frac{m\kappa^2}{H^3}\left(\frac{1}{1+Pr^{-1/2}}\right)^2 \frac{t^2}{t_p} \sim \frac{y}{t}, \tag{26}$$

which implies

$$t^3 \sim \frac{t_p}{\gamma Ra}\frac{H^3 y}{m\kappa^2}(1+Pr^{-1/2})^2, \tag{27}$$

which gives the following scaling for the time when the boundary layer enters into the quasi-steady mode

$$t_0 \sim \frac{1}{(\gamma Ra)^{1/3}}\left(\frac{t_p}{H^2/\kappa}\right)\frac{H^2}{m^{1/3}\kappa}\left(\frac{y}{H}\right)^{1/3}(1+Pr^{-1/2})^{2/3}. \tag{28}$$

The corresponding scaling for the maximum velocity at t_0 from equation (22)

$$v_0 \sim (\gamma Ra)^{1/3}\left(\frac{H^2/\kappa}{t_p}\right)^{1/3}\frac{m^{1/3}\kappa}{H}\left(\frac{y}{H}\right)^{2/3}\left(\frac{1}{1+Pr^{-1/2}}\right)^{2/3}, \tag{29}$$

and the scaling for the thermal boundary layer thickness at the same time from equation (6) is

$$\delta_{T0} \sim \frac{1}{(\gamma Ra)^{1/6}}\left(\frac{t_p}{H^2/\kappa}\right)^{1/6}\frac{H}{m^{1/6}}\left(\frac{y}{H}\right)^{1/6}(1+Pr^{-1/2})^{1/3}. \tag{30}$$

The scaling for the thickness of the viscous layer from the wall to the position where the velocity is maximum at time t_0 from (19) is

$$\delta_{vm0} \sim \frac{1}{(\gamma Ra)^{1/6}}\left(\frac{t_p}{H^2/\kappa}\right)^{1/6}\frac{H}{m^{1/6}}\left(\frac{y}{H}\right)^{1/6}\left(\frac{1}{1+Pr^{-1/2}}\right)^{2/3}. \tag{31}$$

The whole viscous boundary layer thickness at the same time from equation (18) is

$$\delta_{v0} \sim \frac{1}{(\gamma Ra)^{1/6}}\left(\frac{t_p}{H^2/\kappa}\right)^{1/6}\frac{H}{m^{1/6}}\left(\frac{y}{H}\right)^{1/6}Pr^{1/2}(1+Pr^{-1/2})^{1/3}. \tag{32}$$

However, if $t_p > t_0$ then the boundary layer will reach a quasi-steady state mode at t_0 before the ramp is finished and for $t_0 < t < t_p$, the boundary layer will continue to develop, governed by a balance between convection and conduction. Thus, for $t_0 < t < t_p$,

$$v_m \frac{\Delta T}{y}\left(\frac{t}{t_p}\right) \sim \kappa \frac{\Delta T}{\delta_T^2}\left(\frac{t}{t_p}\right), \tag{33}$$

where now δ_T is no longer governed by (6). This gives

$$v_m \sim \frac{\kappa y}{\delta_T^2}. \tag{34}$$

The same balances between buoyancy and viscosity still apply in regions I and II, so that (17) applies. Further, since the boundary layer is in a quasi-steady mode, the balance in region III is between advection and diffusion of momentum, so that

$$v_m \sim \frac{\nu y}{\delta_v^2}, \tag{35}$$

and again $\delta_{vm} \sim \delta_T/(1+Pr^{-1/2})$.

Using this result the velocity given by the balance in region I is

$$v_m \sim \frac{\chi_0(\beta + 1/T_0)\Delta T \delta_T^2}{\nu\mu_m}\left(\frac{t}{t_p}\right)\frac{b^2}{y}\left(\frac{1}{1+Pr^{-1/2}}\right)^2. \tag{36}$$

Together with (36) a δ_T scale may be obtained as

$$\delta_T \sim \frac{H}{(\gamma Ra)^{1/4}} m^{1/4}\left(\frac{y}{H}\right)^{1/2}(1+Pr^{-1/2})^{1/2}\left(\frac{t_p}{t}\right)^{1/4}, \tag{37}$$

and the corresponding scale of V_m.

$$v_m \sim (\gamma Ra)^{1/2} m^{1/2} \left(\frac{\kappa}{H}\right) \frac{1}{1+Pr^{-1/2}} \left(\frac{t_p}{t}\right)^{1/2}. \qquad (38)$$

Corresponding scales for the viscous boundary layer thickness δ_v and the position of the velocity maximum, δ_{vm} are readily obtained. It is seen from (37) and (38) that, in this quasi-steady stage of the boundary layer development, the velocity increases, but the boundary layer thickness decreases with time. At $t \sim t_p$, the boundary layer becomes completely steady state, with thickness δ_{Tp} and velocity v_{mp}, given by

$$\delta_{Tp} \sim \frac{H}{(\gamma Ra)^{1/4}} m^{1/4} \left(\frac{y}{H}\right)^{1/2} (1+Pr^{-1/2})^{1/2}, \qquad (39)$$

and

$$v_{mp} \sim (\gamma Ra)^{1/2} m^{1/2} \frac{\kappa}{H} \frac{1}{1+Pr^{-1/2}}. \qquad (40)$$

Numerical scheme and grid and time step dependence tests

Equations (1) - (4) are solved along with the initial and boundary conditions using the SIMPLE scheme. The Finite Volume Method has been chosen to discretize the governing equations, with the QUICK scheme approximating the advection term. The diffusion terms are discretized using central-differencing with second order accuracy. A second order implicit time-marching scheme has also been used for the unsteady term. Three non-uniform grid sizes, 50×50, 100×100 and 150×150 with coarser grids in the core and finer grids concentrated in the proximity of three walls (except the open end) were constructed for grid dependency test. The time steps were chosen in such a way that the CFL (Courant - Freidrichs - Lewy) number remains the same for all grids. It was found that the maximum error among three grid sizes were less than 2%. For brevity, the test results are not presented here. This means that either grid system is able to capture the flow development and the heat transfer into this system. Therefore, the grid size of 100×100 and the time step of $0.01s$ are adopted for the simulations.

Validation of selected scales

The scaling predictions for magnetic convection of paramagnetic fluids obtained above can be validated and analysed by numerical simulations. For page limitation only one scaling relation is validated here. However, all validation will be shown in the presentation.

The computed velocity is taken along the line perpendicular to the left vertical wall at its mid point, which is sufficiently far from the leading edge. The time series of the maximum velocity parallel to the plate (v_m) has been recorded on this line, which has been used to verify the velocity scaling relation (29). In Fig. 3, the umerically obtained maximum velocities for different values of Ra and Pr for $m = 2$ and $t_p = 8s$ at time t_0 is used along x-axis and the scaling values are used in the corresponding y-axis. It is found that all values lie on a single line, which proves that the scaling relation (29) agrees very well with the numerical results.

Conclusions

Scaling analysis of thermo-magnetic convection in an open squared cavity filled with a paramagnetic fluid of $Pr > 1$ is considered in this study subject to a gradient magnetic field prediction. The detailed scaling results have been presented. However, due to page limitation all scalings are not validated here. Numerical results demonstrate that the scalings accurately represent the physical behaviour of the whole stage of the flow

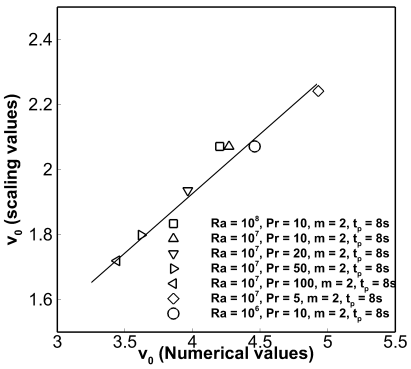

Figure 3: Comparison of maximum velocity calculated at time t_0 from numerical simulations and scaling

development. A three-region structure for the boundary layer is analysed during scaling development which improves scaling predictions for Pr variation. It is clearly shown by scaling that during the start-up stage the boundary-layer development is one-dimensional, independent of height, and becomes two-dimensional and height dependent when the convection starts to dominate the flow.

References

[1] Braithwaite, D., Beaugnon, E. and Tournier, R. Magnetically controlled convection in paramagnetic fluid, *Nature*, **354**, 1991, 667-673.

[2] Kaneda, M., Tagawa, T. and Ozoe, H., Convection induced by a cusp-shaped magnetic field for air in a cube heated from above and cooled from below, *Journal of Heat Transfer*, **124**, 2002, 1725.

[3] Tagawa, T., Ujihara, A. and Ozoe, H., Numerical computation for Rayleigh-Benard convection of water in a magnetic field, *Int. J. Heat Mass Transfer*, **46**, 4097-4104.

[4] Bednarz, T. P., Fornalik, E., Tagawa, T., Ozoe, H. and Szmyd, J. S., Convection of paramagnetic fluid in a cube heated and cooled from side walls and placed below a superconducting magnet comparison between experiment and numerical computations, *Thermal Science & Engineering Journal*, **14**, 2006, 107-114.

[5] Bednarz, T. P., Lin, W., Patterson, J. C., Lei, C. and Armfield, S. W., Scaling for unsteady thermo-magnetic convection boundary layer of paramagnetic fluids of $Pr > 1$ in micro-gravity conditions, *Int. J. Heat Fluid Flow*, **30**, 2009, 1157-1170.

[6] Saha, S. C., Patterson, J. C. and Lei, C. Natural convection in attic-shaped spaces subject to sudden and ramp heating boundary conditions, *Heat Mass Transfer*, **46**, 2010a, 621–638.

[7] Saha, S. C., Patterson, J. C. and Lei, C. Natural convection and heat transfer in attics subject to periodic thermal forcing, *Int. J. Therm. Sci.*, **49**, 2010b, 1899–1910.

[8] Saha, S. C., Patterson, J. C. and Lei, C. Natural convection in attics subject to instantaneous and ramp cooling boundary conditions, *Energy Buildings*, **42**, 2010c, 1192–1204.